Available online at www.sciencedirect.com

ScienceDirect

Journal of Sound and Vibration 322 (2009) 15–28

JOURNAL OF SOUND AND VIBRATION

www.elsevier.com/locate/jsvi

Influence of tire damping on mixed $\mathscr{H}_2/\mathscr{H}_\infty$ synthesis of half-car active suspensions☆

Hüseyin Akçay*, Semiha Türkay

Department of Electrical and Electronics Engineering, Anadolu University, 26470 Eskişehir, Turkey

Received 13 July 2008; received in revised form 28 September 2008; accepted 5 November 2008
Handling Editor: J. Lam
Available online 20 December 2008

Abstract

In this paper, multi-objective control of a half-car suspension system using linear matrix inequalities is studied. It is observed that when tire damping is precisely known, road-holding quality of the suspension system can be improved to some extent by the design procedure while ride comfort and compactness of suspension rattling space are only slightly affected as tire damping coefficients are increased. In the absence of tire damping information, a robust controller is designed for a suspension system with polytopic tire damping uncertainties. In contrast to multi-objective control of quarter-car models with polytopic tire damping uncertainties, this robust design does not offer any advantage over an active suspension system designed by neglecting tire damping. The results, based on the assumption that the front and the rear road velocity inputs are uncorrelated white-noise processes, demonstrate that the body pitch significantly impacts the closed-loop performance of the active suspension system. This implies that decomposition of a half-car model into two independent quarter-car models by a linear transformation is not realistic for a study of the performance limitations and the trade-offs.

1. Introduction

In the automotive industry, there is considerable interest for the development of active and semi-active suspensions, which can significantly improve both vehicle ride and handling when compared to conventional passive suspensions [1–8]. From the early 1960s, starting with simple quarter-car models, optimal control theory was used to establish the potential benefits of active suspension systems. Constraints and trade-offs on achievable performances have also been studied [9–14].

In Refs. [10,11], constraints on achievable frequency responses were derived from an invariant point perspective. A mechanical multi-port network approach was developed in Ref. [13] to study the performance capabilities and constraints. In Refs. [13,14], for a quarter-car model of an automotive suspension a complete set of constraints on several transfer functions of interest from the road and the load disturbances were derived

☆This work was supported by the Scientific and Technological Research Council of Turkey under Grant 106E108.
*Corresponding author. Tel.: +90 222 3350580; fax: +90 222 3239501.
E-mail address: huakcay@anadolu.edu.tr (H. Akçay).

0022-460X/$ - see front matter
doi:10.1016/j.jsv.2008.11.007

by making use of the factorization approach to feedback stability and the Youla parameterization of stabilizing controllers. These constraints typically arise in the form of finite and non-zero invariant frequency points and the growth restrictions on the frequency responses and derivatives at zero and infinite frequencies.

In most works, tire damping is neglected when modeling automotive active suspension systems. This is partly due to the fact that tire damping is difficult to estimate since it depends on many factors i.e., size, applied pressure, free or rotating, new or worn, all season or snow, etc. [15,16]. In fact, tire damping by itself has little influence on the wheel-hop vibration since this mode is mainly damped by the shock absorber. The ignorance of damping in tire models compelled misleading conclusion that at the wheel-hop frequency, motions of the sprung and unsprung masses are uncoupled, and the vertical acceleration of the sprung mass will be unaffected [10,11]. For a two-degree-of-freedom quarter-car model, it is pointed out in Ref. [17] that by taking tire damping to be small but non-zero, these motions become coupled at all frequencies, and control forces can be used to reduce the sprung mass vertical acceleration at the wheel-hop frequency. The effect of introducing tire damping can be quite large [14].

The study of the constraints on the achievable performance has remained largely restricted to pointwise constraints in the frequency domain (and quarter-car models) while ride comfort and safety criteria are mostly expressed in terms of the root-mean-square (rms) values of the sprung mass vertical acceleration, the suspension travels, and the tire deflections. It is generally agreed that typical road surfaces may be considered as realizations of homogeneous and isotropic two-dimensional Gaussian random processes and these assumptions make it possible to completely describe a road profile by a single power spectral density evaluated from any longitudinal track. Then, the spectral description of the road, together with a knowledge of traversal velocity and of the dynamic properties of the vehicle, provide a response analysis which will describe the response of the vehicle expressed in terms of displacement, acceleration, or stress.

This paper is organized as follows. In Section 2, a four-degree-of-freedom half-car model is reviewed. In Section 3, first, assuming that tire damping is known, a multi-objective suspension control problem is formulated and solved by using linear matrix inequalities. The control objective is to decrease the rms vertical and the pitch accelerations while keeping the rms gain of the suspension travels bounded. This is the well-known ride comfort-road-holding trade-off experienced in the design of active suspension systems. The influence of tire damping on the solution of this optimization problem is studied; it is observed that tire damping affects only the road-holding quality while the remaining responses are insensitive to changes of tire damping coefficients in the range considered. Next, in Section 3.2, the assumption that tire damping coefficients are known is dropped and a multi-objective control problem for suspension models with tire damping coefficients confined to a prescribed box is formulated. By using linear matrix inequalities, a robust controller with guaranteed performance over all suspension models in the uncertainty set is obtained. The closed-loop performance of the designed suspension system is studied; and it is found that this robust controller does not offer any advantage over an active suspension system designed by neglecting tire damping. The paper is concluded by Section 4.

Multi-objective control of vehicle suspensions by using linear matrix inequalities is not new. In Ref. [8], a constrained $\mathscr{H}_\infty$ control scheme with output and control constraints were studied. In Ref. [18], problems with $\mathscr{H}_2$ or $\mathscr{H}_\infty$ cost under positive realness constraint on controller structures were considered. The control objectives similar to those in this paper were studied in Ref. [19]. Robust multi-objective controllers were synthesized in Refs. [20,21] to cope with parameter uncertainties in system matrices characterized by a given polytope.

2. The half-car model

A four degree-of-freedom half-car model is shown in Fig. 1. In this model, the car body is represented by the sprung mass m_s and the pitch moment of inertia I_p, and the front and the rear wheels are represented by the unsprung masses m_{u1} and m_{u2}, respectively. The suspension system consists of two actuators u_1 and u_2 in parallel with the linear passive suspension elements k_{s1} and c_{s1} and k_{s2} and c_{s2}. Each tire is modeled by a simple linear spring k_{t1} or k_{t2} in parallel with a linear damping element c_{t1} or c_{t2}. The variables x_G and θ stand for the vertical displacement at the center of gravity and the pitch angle of the sprung mass, respectively. The front and the rear road disturbances and their time derivatives are denoted, respectively, by w_1, w_2, v_1, v_2 and the

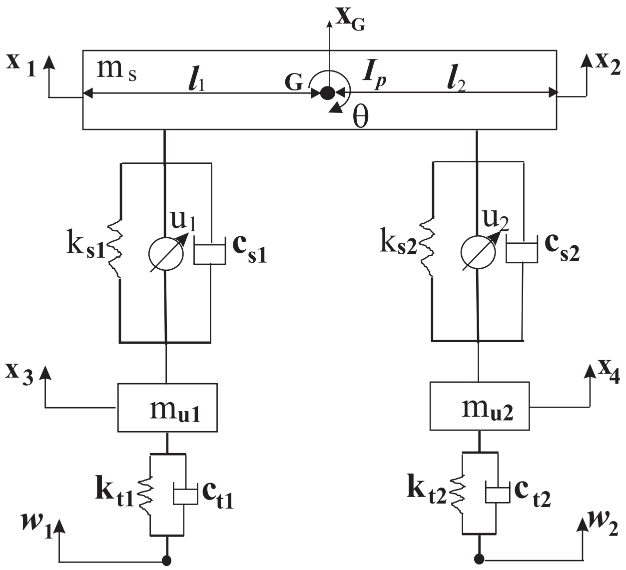

Fig. 1. The half-car model of the vehicle.

Table 1
The vehicle system parameters for the half-car model.

Sprung mass	m_s	500 kg
Pitch moment of inertia	I_p	2700 kg m^2
Unsprung masses	m_{u1}, m_{u2}	36 kg
Damping coefficients	c_{s1}, c_{s2}	980 N s m^{-1}
Suspension stiffnesses	k_{s1}, k_{s2}	16,000 N m^{-1}
Tire stiffnesses	k_{t1}, k_{t2}	160,000 N m^{-1}
Distance of front axle to sprung mass c.g.	l_1	1.5 m
Distance of rear axle to sprung mass c.g.	l_2	2.5 m

control inputs are the actuator forces u_1 and u_2. The variables x_1, x_2, x_3, x_4, w_1, and w_2 are measured with respect to an inertial frame. The parameter values which are typical for a lightly damped passenger car, except c_{t1} and c_{t2}, chosen for this study are shown in Table 1.

Assuming that the tires behave as point-contact followers that are in contact with the road at all times, the equations of motion take the following form:

$$m_s\ddot{x}_G = -k_{s1}(x_1 - x_3) - c_{s1}(\dot{x}_1 - \dot{x}_3) - k_{s2}(x_2 - x_4) - c_{s2}(\dot{x}_2 - \dot{x}_4) - u_1 - u_2, \tag{1}$$

$$I_p\ddot{\theta} = -l_1k_{s1}(x_1 - x_3) - l_1c_{s1}(\dot{x}_1 - \dot{x}_3) + l_2k_{s2}(x_2 - x_4) + l_2c_{s2}(\dot{x}_2 - \dot{x}_4) - l_1u_1 + l_2u_2, \tag{2}$$

$$m_{u1}\ddot{x}_3 = k_{s1}(x_1 - x_3) + c_{s1}(\dot{x}_1 - \dot{x}_3) + u_1 - k_{t1}(x_3 - w_1) - c_{t1}(\dot{x}_3 - \dot{w}_1), \tag{3}$$

$$m_{u2}\ddot{x}_4 = k_{s2}(x_2 - x_4) + c_{s2}(\dot{x}_2 - \dot{x}_4) + u_2 - k_{t2}(x_4 - w_2) - c_{t2}(\dot{x}_4 - \dot{w}_2). \tag{4}$$

The displacements at the front and the rear wheels of the vehicle are related to x_G and θ by

$$\begin{bmatrix} x_1 \\ x_2 \end{bmatrix} = \mathbf{S}\begin{bmatrix} x_G \\ \theta \end{bmatrix},$$

where

$$\mathbf{S} = \begin{bmatrix} 1 & l_1 \\ 1 & -l_2 \end{bmatrix}.$$

It will be more convenient to define a new set of state variables in terms of the old state variables and the disturbances as follows:

$$\tilde{x}_1 = x_1 - x_3, \quad \tilde{x}_2 = x_2 - x_4, \quad \tilde{x}_3 = x_3 - w_1, \quad \tilde{x}_4 = x_4 - w_2,$$
$$\tilde{x}_5 = \dot{x}_1, \quad \tilde{x}_6 = \dot{x}_2, \quad \tilde{x}_7 = \dot{x}_3, \quad \tilde{x}_8 = \dot{x}_4. \tag{5}$$

Let

$$\mathbf{u} = [u_1 \;\; u_2]^{\mathrm{T}},$$
$$\mathbf{w} = [w_1 \;\; w_2]^{\mathrm{T}},$$
$$\mathbf{v} = [v_1 \;\; v_2]^{\mathrm{T}},$$
$$\mathbf{M}_s = \mathrm{diag}(m_s, I_p),$$
$$\mathbf{K}_s = \mathrm{diag}(k_{s1}, k_{s2}),$$
$$\mathbf{C}_s = \mathrm{diag}(c_{s1}, c_{s2}),$$
$$\mathbf{M}_u = \mathrm{diag}(m_{u1}, m_{u2}),$$
$$\mathbf{K}_t = \mathrm{diag}(k_{t1}, k_{t2}),$$
$$\mathbf{C}_t = \mathrm{diag}(c_{t1}, c_{t2}),$$

where the MATLAB notation is adopted. Then, the equations of motion can be put into the state-space form

$$\dot{\tilde{\mathbf{x}}} = \mathbf{A}\tilde{\mathbf{x}} + \mathbf{B}_1\mathbf{v} + \mathbf{B}_2\mathbf{u}, \tag{6}$$

where

$$\mathbf{A} = \begin{bmatrix} \mathbf{0}_{4\times4} & \begin{matrix} \mathbf{I}_2 & -\mathbf{I}_2 \\ \mathbf{0}_{2\times2} & \mathbf{I}_2 \end{matrix} \\ \mathbf{K} & \mathbf{C} \end{bmatrix}, \tag{7}$$

$$\mathbf{B}_1 = \begin{bmatrix} \mathbf{0}_{2\times2} \\ -\mathbf{I}_2 \\ \mathbf{N} \end{bmatrix},$$

$$\mathbf{B}_2 = \begin{bmatrix} \mathbf{0}_{4\times2} \\ \mathbf{W} \end{bmatrix},$$

$$\mathbf{K} = -\begin{bmatrix} \mathbf{S}\mathbf{M}_s^{-1}\mathbf{S}^{\mathrm{T}}\mathbf{K}_s & \mathbf{0}_{2\times2} \\ -\mathbf{M}_u^{-1}\mathbf{K}_s & \mathbf{M}_u^{-1}\mathbf{K}_t \end{bmatrix},$$

$$\mathbf{C} = -\begin{bmatrix} \mathbf{S}\mathbf{M}_s^{-1}\mathbf{S}^{\mathrm{T}}\mathbf{C}_s & \mathbf{0}_{2\times2} \\ -\mathbf{M}_u^{-1}\mathbf{C}_s & \mathbf{M}_u^{-1}(\mathbf{C}_s + \mathbf{C}_t) \end{bmatrix},$$

$$\mathbf{N} = \begin{bmatrix} \mathbf{0}_{2\times2} \\ \mathbf{M}_u^{-1}\mathbf{C}_t \end{bmatrix},$$

$$\mathbf{W} = \begin{bmatrix} -\mathbf{S}\mathbf{M}_s^{-1}\mathbf{S}^{\mathrm{T}} \\ \mathbf{M}_u^{-1} \end{bmatrix}, \tag{8}$$

and $\mathbf{0}_{m\times n}$ and $\mathbf{I}_n$ denote, respectively, m by n matrix of zeros and the n by n identity matrix.

The objective of this paper is to study the multi-objective control of a half-car active suspension system excited by random road disturbances. The vehicle response variables that need to be examined are the heave and the pitch accelerations of the sprung mass as indicators of the vibration isolation, the suspension travels as measures of the rattling space, and the tire deflections as indicators of the road-holding characteristic of the vehicle. These variables stacked in the variable $\mathbf{z}$ can be written in terms of the state variables and the control inputs as

$$\mathbf{z} = (\tilde{x}_1 \;\; \tilde{x}_2 \;\; \tilde{x}_3 \;\; \tilde{x}_4 \;\; \ddot{x}_G \;\; \ddot{\theta})^{\mathrm{T}}. \tag{9}$$

By using state-space parameters, $\mathbf{z}$ can be written compactly as follows:

$$\mathbf{z} = \mathbf{C}_1\tilde{\mathbf{x}} + \mathbf{D}_1\mathbf{u}, \tag{10}$$

where

$$\mathbf{C}_1 = \begin{bmatrix} \mathbf{I}_4 & \mathbf{0}_{4\times 4} \\ -\mathbf{M}_s^{-1}\mathbf{S}^{\mathrm{T}}[\mathbf{K}_s \;\; \mathbf{0}_{2\times 2} \;\; \mathbf{C}_s] & \mathbf{0}_{2\times 2} \end{bmatrix},$$

$$\mathbf{D}_1 = \begin{bmatrix} \mathbf{0}_{4\times 2} \\ -\mathbf{M}_s^{-1}\mathbf{S}^{\mathrm{T}} \end{bmatrix}.$$

For the design of a feedback law, the suspension travel measurements:

$$\mathbf{y} = \mathbf{C}_2\hat{\mathbf{x}} \tag{11}$$

will be considered where

$$\mathbf{C}_2 = [\mathbf{I}_2 \;\; \mathbf{0}_{2\times 6}].$$

The derivative of the road roughness is most commonly specified as a random process $\mu\sqrt{V}\eta(t)$ where V is the vehicle's forward velocity, μ is the road roughness coefficient, and $\eta(t)$ is unit-intensity white-noise process. In this study, V and μ are fixed as $V = 20\,\mathrm{m/s}$ and $\mu = 0.0027$. Thus, the covariance function of $\mathbf{v}$ denoted by $\mathbf{R}_\mathbf{v}$ satisfies

$$\mathbf{R}_\mathbf{v}(\tau) = \mu^2 V\mathbf{I}_2\delta(\tau), \tag{12}$$

where $\delta(\tau)$ is the unit impulse function.

Passenger comfort requires the rms body accelerations be as small as possible while compactness of the rattle space, good handling characteristics, and improved road-holding quality require the suspension travels and the tire deflections to be kept as small as possible. It is a well-known fact [9] that these objectives cannot be met simultaneously with a passive suspension system.

3. Multi-objective control of vehicle suspension systems

The primary goal of active suspension design is to improve ride comfort by making the heave and the pitch accelerations of the car body as small as possible while keeping the suspension travels below the maximum allowable suspension stroke to prevent excessive suspension bottoming, which can result in structural damage and deterioration of ride comfort. The dynamic tire loads should not exceed the static ones in order to ensure a firm uninterrupted contact of wheels to road. Meanwhile, active forces should be amplitude bounded to avoid actuator saturations. Thus, the design of active suspension system is a multi-objective control problem in which the strategy is to reduce the accelerations while keeping the constraints satisfied. Many other constraints can also be taken into consideration. However, the above constraints reveal all fundamental design trade-offs.

In this paper, first the following dynamic output feedback structure:

$$\dot{\mathbf{x}}_c = \mathbf{A_F}\mathbf{x}_c + \mathbf{B_F}\mathbf{y}, \tag{13}$$

$$\mathbf{u} = \mathbf{C_F}\mathbf{x}_c + \mathbf{D_F}\mathbf{y} \tag{14}$$

will be considered where the state-space parameters $\mathbf{A_F}$, $\mathbf{B_F}$, $\mathbf{C_F}$, $\mathbf{D_F}$ of the transfer matrix: $\mathbf{F}(s) = \mathbf{C_F}(s\mathbf{I} - \mathbf{A_F})^{-1}\mathbf{B_F} + \mathbf{D_F}$ are to be determined. The feedback configuration of the generalized plant defined by

$$\mathbf{G}(s) = \left[\begin{array}{c|c} \mathbf{G}_{11} & \mathbf{G}_{12} \\ \hline \mathbf{G}_{21} & \mathbf{G}_{22} \end{array}\right] \tag{15}$$

which maps the pair of inputs $[\mathbf{v}^{\mathrm{T}}\ \mathbf{u}^{\mathrm{T}}]^{\mathrm{T}}$ to the pair of outputs $[\mathbf{z}^{\mathrm{T}}\ \ \mathbf{y}^{\mathrm{T}}]^{\mathrm{T}}$ and $\mathbf{F}(s)$ is shown in Fig. 2.

Let $\mathbf{T_{zv}}(s)$ denote the closed-loop transfer function from $\mathbf{v}$ to $\mathbf{z}$. The design specifications mentioned above can be cast into the optimization problem:

$$\mathscr{J}(\Lambda) = \min_{\mathbf{F}\in\mathscr{RH}_\infty} \|\mathbf{\Lambda}\mathbf{T_{zv}}\|_2^2, \tag{16}$$

where $\mathscr{RH}_\infty$ is the set of real-rational transfer matrices which are analytic on the closed-right half-plane and the weighting matrix $\mathbf{\Lambda} = \mathrm{diag}(\Lambda_1, \ldots, \Lambda_6)$ has non-negative entries. Note from the definition of the $\mathscr{H}_2$-norm and the fact that the power spectrum of $\mathbf{v}$ denoted by $\mathscr{S}_{\mathbf{v}}(\mathrm{j}\omega)$ satisfies $\mathscr{S}_{\mathbf{v}}(\mathrm{j}\omega) = \mu^2 V\mathbf{I}_2$ for all ω, Eq. (16) can be written as

$$\begin{aligned}
\mathscr{J}(\mathbf{\Lambda}) &= \min_{\mathbf{F}\in\mathscr{RH}_\infty} \frac{1}{2\pi}\int_{-\infty}^{\infty} \mathrm{Tr}\{\mathbf{\Lambda}\mathbf{T_{zv}}(\mathrm{j}\omega)\mathbf{T}^{\sim}_{\mathbf{zv}}(\mathrm{j}\omega)\mathbf{\Lambda}\}\,\mathrm{d}\omega \\
&= (\mu^2 V)^{-1} \min_{\mathbf{F}\in\mathscr{RH}_\infty} \sum_{k=1}^{6} \frac{\Lambda_k^2}{2\pi}\int_{-\infty}^{\infty} \mathbf{T}^{\sim}_{z_k\mathbf{v}}(\mathrm{j}\omega)\mathscr{S}_{\mathbf{v}}(\mathrm{j}\omega)\mathbf{T}_{z_k\mathbf{v}}(\mathrm{j}\omega)\,\mathrm{d}\omega \\
&= (\mu^2 V)^{-1} \min_{\mathbf{F}\in\mathscr{RH}_\infty} \sum_{k=1}^{6} \Lambda_k^2\,\mathrm{E}[z_k]^2,
\end{aligned}$$

where $\mathbf{H}^{\sim}(s) = \mathbf{H}^{\mathrm{T}}(-s)$, $\mathrm{E}(a)$ is the expected value of a given random variable a, and $\mathrm{Tr}(\mathbf{X})$ denotes the trace of a given square matrix $\mathbf{X}$. Hence, the optimal control inputs minimize a weighted combination of the squared rms values of the outputs.

By allowing only a few of the weights in Eq. (16) to be non-zero, it is conceivable to make the heave and the pitch accelerations of the body arbitrarily close to zero at the expense of increasing the suspension travels and the tire deflections. To respect the trade-offs, in Eq. (16) non-zero weights are assigned to the suspension travels. In addition, an rms gain constraint on the tire deflections:

$$\|\mathscr{W}\mathbf{T_{zv}}\|_\infty < \gamma, \quad \gamma > 0, \tag{17}$$

where $\mathscr{W} = \mathrm{diag}(\mathbf{0}_{2\times 2}, \mathbf{I}_2, \mathbf{0}_{2\times 2})$ is imposed and $\Lambda_3 = \Lambda_4 = 0$ is set in Eq. (16). This rms gain constraint shapes the optimal solution. The multi-objective control design problem can be summarized as follows:

For given numbers $\gamma > 0$, $\Lambda_k = 0$ for $k = 3, 4$ and $\Lambda_k > 0$ otherwise, design an output-feedback controller $\mathbf{u} = \mathbf{F}(s)\mathbf{y}$ that satisfies $\|\mathscr{W}\mathbf{T_{zv}}\|_\infty < \gamma$ and minimizes $\|\mathbf{\Lambda}\mathbf{T_{zv}}\|_2^2$.

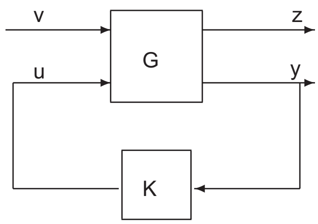

Fig. 2. Standard block diagram.

Some control design requirements were expressed in the time domain. The multi-objective control problem, on the other hand, has the control objective and the constraint in the frequency domain. A linear matrix inequality based solution will be presented. This formalism readily encompasses time-domain constraints at a price of conservatism. By tuning the parameters γ and $\mathbf{\Lambda}$, the solution of the above design problem can be adjusted to satisfy time-domain constraints. In the next subsection, guidelines will be provided how to choose these tuning parameters.

3.1. A linear matrix inequality based solution

Let $\mathbf{G}_{z_k\mathbf{v}}$ denote the open-loop transfer function from $\mathbf{v}$ to z_k, i.e., the kth row of $\mathbf{G}_{11}$ in Eq. (15). The weighting matrix $\mathbf{\Lambda}$ and the upper bound γ of the multi-objective control problem are chosen as follows. In Eqs. (3) and (4), assume c_{t1} is equal to c_{t2} and denote the common value by c_t. Then, given c_t compute $\|\mathbf{G}_{z_k\mathbf{v}}\|_2$ for $k = 1, 2, 5, 6$ and $\|\mathscr{W}\mathbf{G}_{11}\|_\infty$. Now, for some positive parameters ρ_1 and ρ_2 set $\Lambda_k = \|\mathbf{G}_{z_k\mathbf{v}}\|_2^{-1}\rho_1$ for $k = 1, 2$, $\Lambda_k = \|\mathbf{G}_{z_k\mathbf{v}}\|_2^{-1}$ for $k = 5, 6$, and $\gamma = \|\mathscr{W}\mathbf{G}_{11}\|_\infty\rho_2$. By these scalings, the solution of the optimization problem can be monitored with respect to the passive suspension. The parameter ρ_1 controls the trade-offs between the suspension travels and the sprung mass accelerations while ρ_2 controls the trade-offs between the tire deflections and the sprung mass accelerations. The optimization algorithm is implemented by the `hinfmix` command of MATLAB's LMI Control Toolbox [22]. This command produces a controller of degree which is equal to that of the plant.

In Figs. 3 and 4, the rms values of z_k, $k = 1, \ldots, 6$ of a vehicle traveling with a speed of 20 m/s subjected to white-noise velocity excitations are plotted as functions of tire damping coefficient for both the passive and the active suspension systems designed with $\rho_1 = 0.1$ and $\rho_2 = 1.5$ using the suspension travel measurements. As expected, the trade-offs among the vertical acceleration, the pitch acceleration, the suspension travels, and the

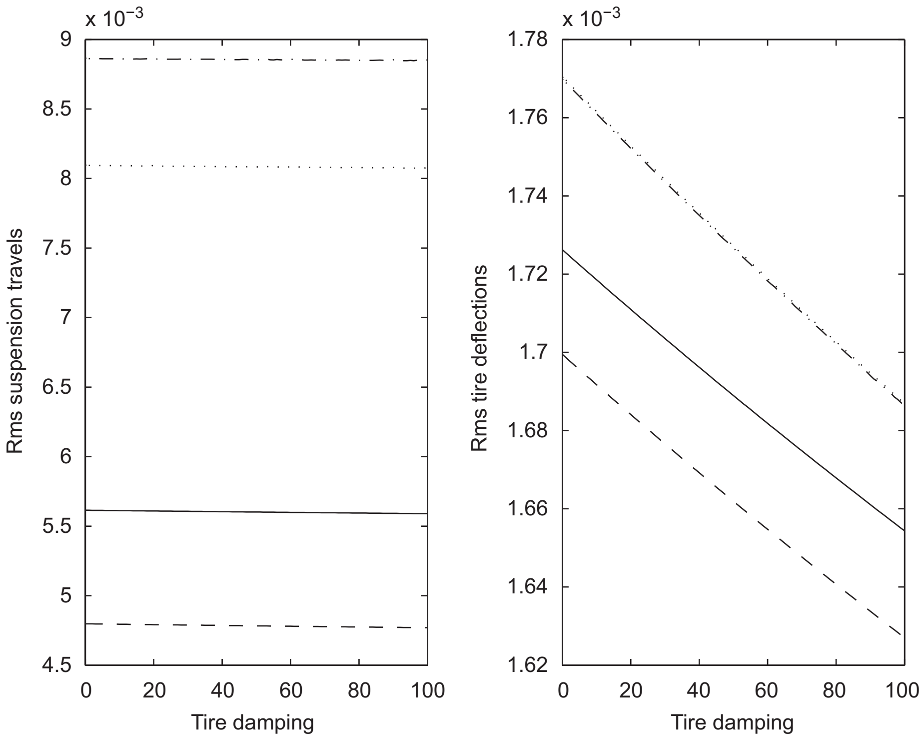

Fig. 3. The rms values of the suspension travels and the tire deflections of the vehicle subjected to white-noise velocity road inputs as functions of c_t: (-) passive suspension (front); (- -) passive suspension (rear); (-.) active suspension (front); (:) active suspension (rear) with $\rho_1 = 0.1$ and $\rho_2 = 1.5$ using the suspension travel measurements.

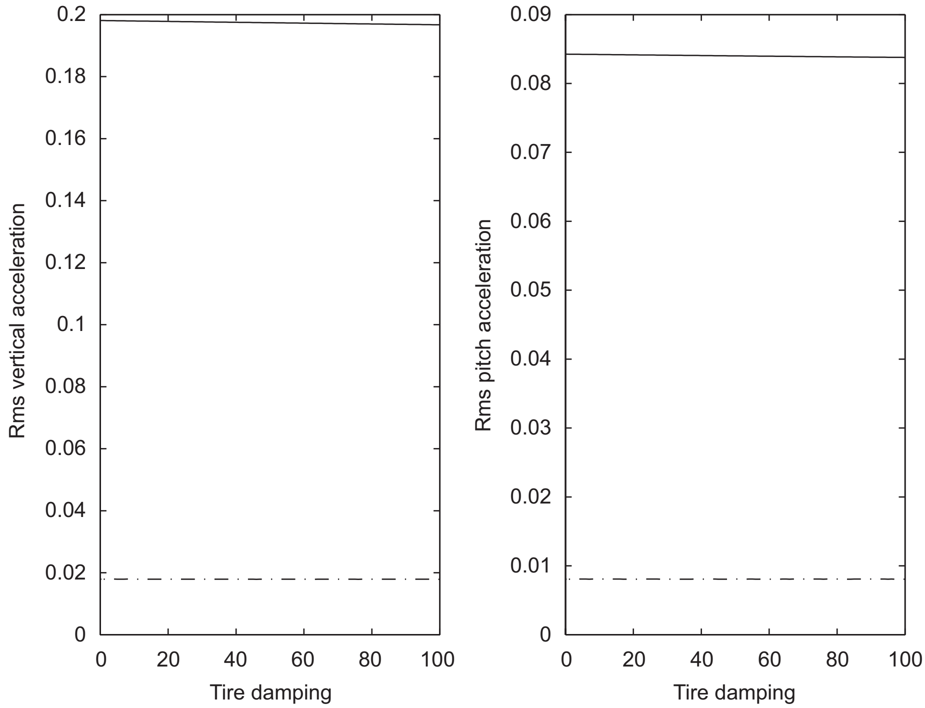

Fig. 4. The rms values of the vertical and the pitch accelerations of the vehicle subjected to white-noise velocity road inputs as functions of c_t: (-) passive suspension; (-.) active suspension with $\rho_1 = 0.1$ and $\rho_2 = 1.5$ using the suspension travel measurements.

tire deflections are notable. In particular, both the vertical and the pitch accelerations are dramatically reduced while the suspension travels are increased by about 60% and the rms tire deflections are slightly increased by about 4%. The rms values of u_1 and u_2 plotted in Fig. 6 for $0 \leqslant c_t \leqslant 100$ show that actuator saturations are not likely to occur. In Fig. 5, the rms gain of the tire deflections is plotted versus tire damping. The rms gain was computed with the formula $\|\mathscr{W}\mathbf{T}_{\mathbf{zw}}\|_\infty$ instead of $\|\mathscr{W}\mathbf{T}_{\mathbf{zv}}\|_\infty$ since the former more realistically quantifies tire deflection sensitivity to road roughness. The rms values and the rms gain of the tire deflections decrease both for the passive and the active suspensions as tire damping is increased from 0 to 100 while the remaining responses decrease very slowly. In fact, the decreases by percentage are 4.1 and 4.2 for the rms passive suspension tire deflections (front and rear), 4.7 and 4.9 for the rms active suspension tire deflections (front and rear), 8.7 for the rms gain of the passive suspension tire deflections, 9.0 for the rms gain of the active suspension tire deflections, 0.4 and 0.6 for the rms passive suspension travels (front and rear), 0.15 and 0.2 for the rms active suspension travels (front and rear), 0.7 for the passive suspension rms vertical acceleration, 0.2 for the active suspension rms vertical acceleration, 0.6 for the passive suspension rms pitch acceleration, and 0.07 for the active suspension rms pitch acceleration (Fig. 6).

To improve the suspension travel and the tire deflection responses, this design procedure is next repeated with $\rho_1 = 1$ and $\rho_2 = 1$. From Figs. 7 and 8, it is seen that the rms values of the suspension travels, the tire deflections, the vertical and the pitch accelerations are reduced by about 12%, 3%, 50%, and 45%, respectively, with respect to the passive suspension. From Fig. 9, the rms gain of the tire deflections is seen to be reduced by about 4% in comparison to the passive suspension. Note from Fig. 10 that the rms values of the control inputs are about 40% of the rms values in the previous case. Thus, the new design is clearly better than the previous one. As noted earlier, only road-holding quality is notably influenced by tire damping. As a matter of fact, the decreases by percentage are 4.1 and 4.2 for the rms passive suspension tire deflections (front and rear), 4.0 and 4.0 for the rms active suspension tire deflections (front and rear), 8.7 for the rms gain of the passive suspension tire deflections, 8.0 for the rms gain of the active suspension tire deflections, 0.4 and 0.6 for the rms passive suspension travels (front and rear), 0.5 and 0.7 for the rms active suspension travels (front and rear), 0.7 for the passive suspension rms vertical acceleration, 0.6 for the active suspension rms vertical

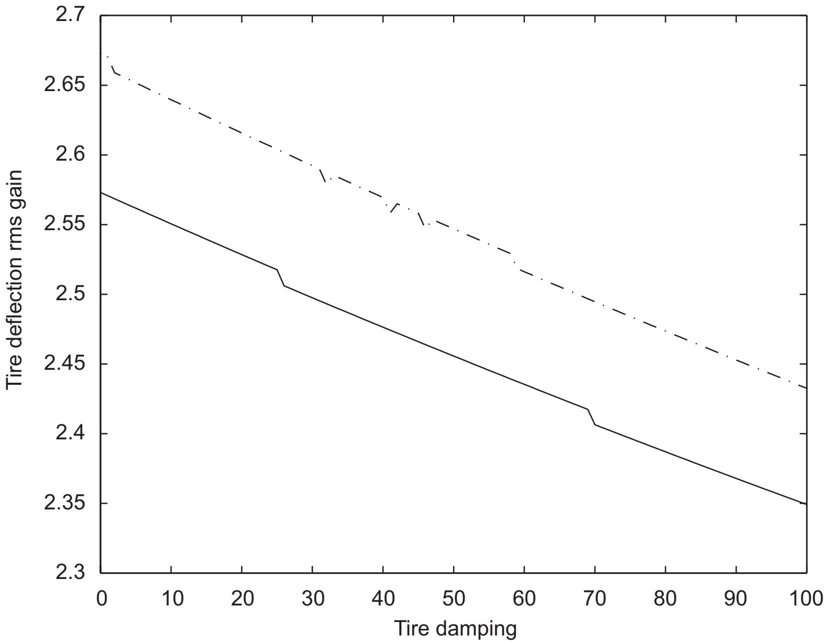

Fig. 5. $\|\mathscr{W}\mathbf{T_{zw}}\|_\infty$ as a function of c_t: (-) passive suspension; (-.) active suspension with $\rho_1 = 0.1$ and $\rho_2 = 1.5$ using the suspension travel measurements.

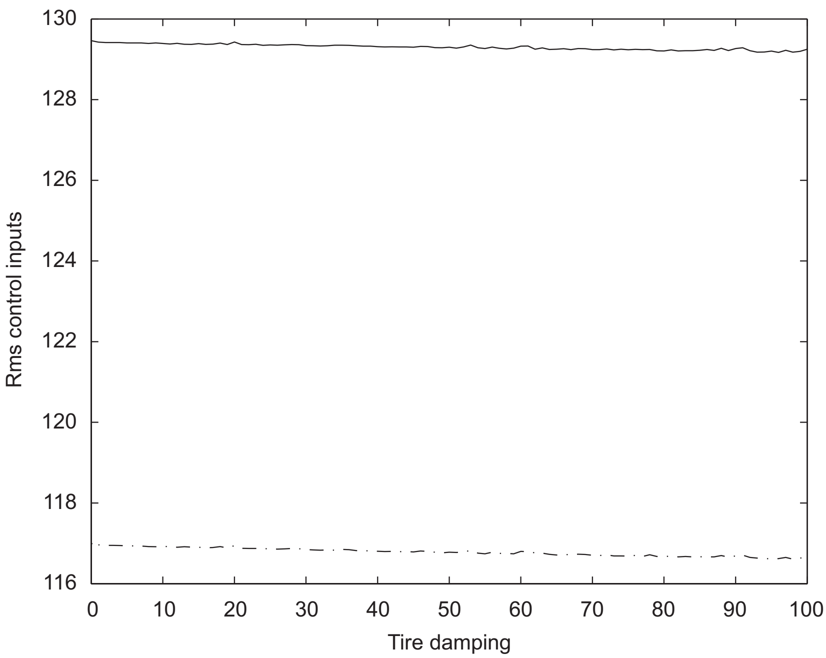

Fig. 6. The rms values of the actuator forces as functions of c_t: (-) u_1; (-.) u_2 with $\rho_1 = 0.1$ and $\rho_2 = 1.5$ using the suspension travel measurements.

acceleration, 0.6 for the passive suspension rms pitch acceleration, and 0.45 for the active suspension rms pitch acceleration.

Based on these observations, it can safely be said that, with the half-car model and the road excitation model in Eq. (12) only road-holding quality is influenced to some extent by tire damping in both the passive

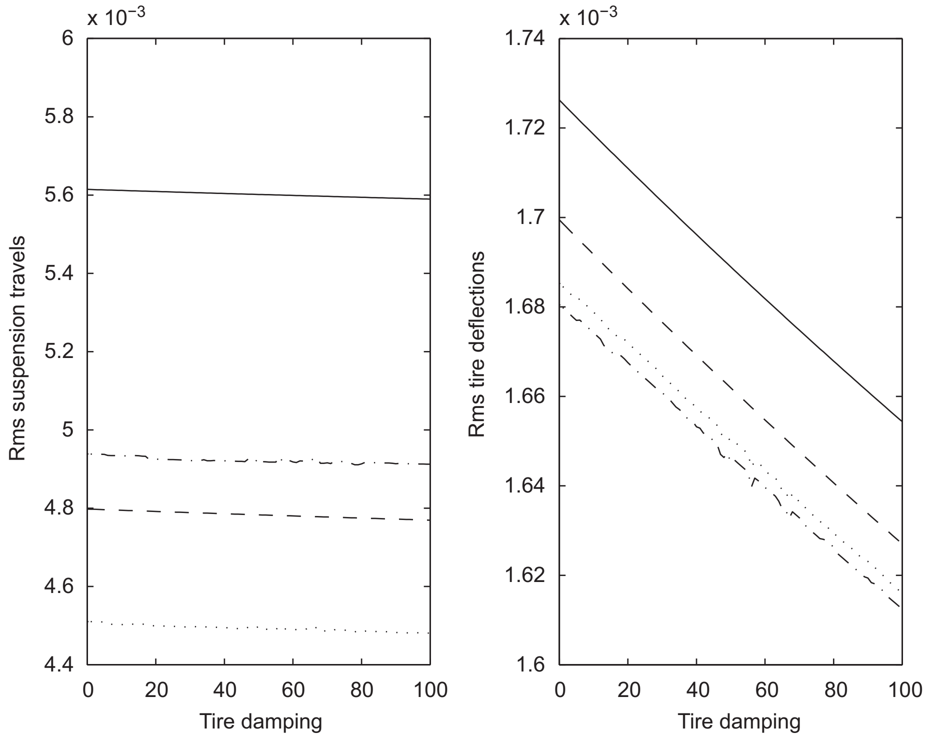

Fig. 7. The rms values of the suspension travels and the tire deflections of the vehicle subjected to white-noise velocity road inputs as functions of c_t: (-) passive suspension (front); (- -) passive suspension (rear); (-.) active suspension (front); (:) active suspension (rear) with $\rho_1 = 1$ and $\rho_2 = 1$ using the suspension travel measurements.

and the active suspension systems. The influence of tire damping on a quarter-car model was investigated in Ref. [23] and it was observed that tire damping significantly reduced all the rms values and the tire deflection rms gains both for the active and the passive suspensions.

It should be noted that the above conclusion was drawn explicitly for the road excitation model in Eq. (12). As the vehicle travels straight on random road profile with a constant forward velocity V a correlation between the front and the rear inputs of the vehicle is induced. The rear wheel is subject to the same road input as the front wheel; but with a time delay T_d:

$$w_2(t) = w_1(t - T_d), \tag{18}$$

where $T_d = (l_1 + l_2)/V$ and $(l_1 + l_2)$ is the wheel base of the vehicle. For control purposes, the pure time delay between the front and the rear inputs may be represented by a finite-dimensional (Pade) approximation. Then, $w_2(t)$ disappears as a variable and the problem can be treated in the same way as in the single input case, as far as the rms responses of the vehicle are concerned. A second-order Pade approximation is accurate enough since the vehicle frequency responses and measured road spectra quickly roll off. In Ref. [24], assuming that the road excitation at the front wheel is modeled by a first-order linear shape filter driven by white-noise input and the excitation at the rear wheel is as in Eq. (18), analogous results to Ref. [23] were obtained.

The excitation model in Eq. (12) presumes that the velocities v_1 and v_2 are uncorrelated. This assumption is hardly justifiable; however, it guarantees simultaneous excitation of the heave and the pitch motions of the car body. The results in this section show that the body pitch significantly impacts the closed-loop performance of the active suspension system. In other words, decomposition of a half-car model into two independent quarter-car models by a linear transformation is not realistic for a study of the performance limitations and the trade-offs.

The multi-objective control problem and consequently its solution depend on the uncertain parameters c_{t1} and c_{t2}. The purpose of this subsection was to examine the influence of tire damping on active suspension

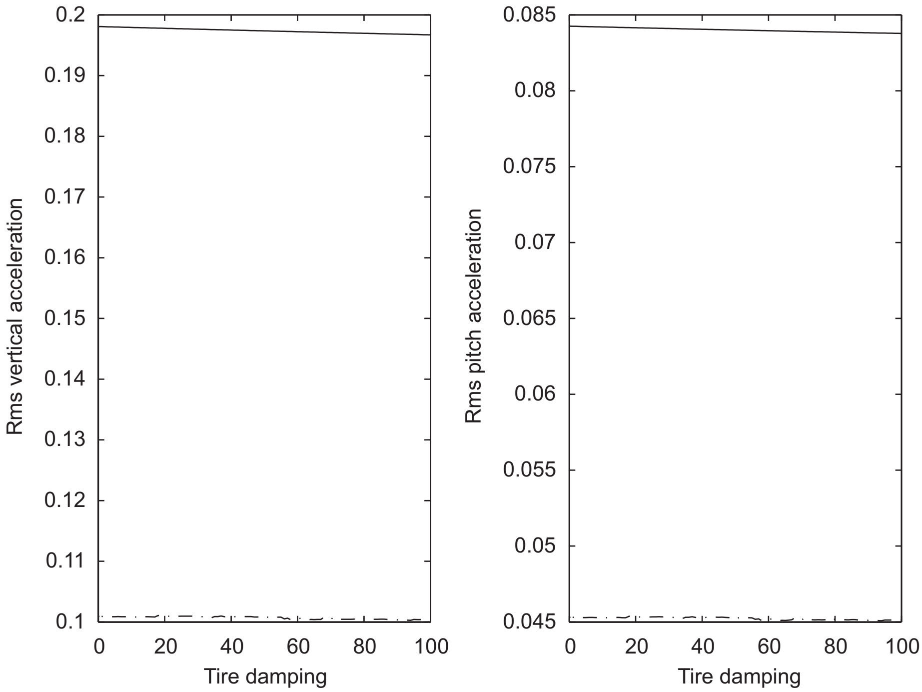

Fig. 8. The rms values of the vertical and the pitch accelerations of the vehicle subjected to white-noise velocity road inputs as functions of c_t: (-) passive suspension; (-.) active suspension with $\rho_1 = 1$ and $\rho_2 = 1$ using the suspension travel measurements.

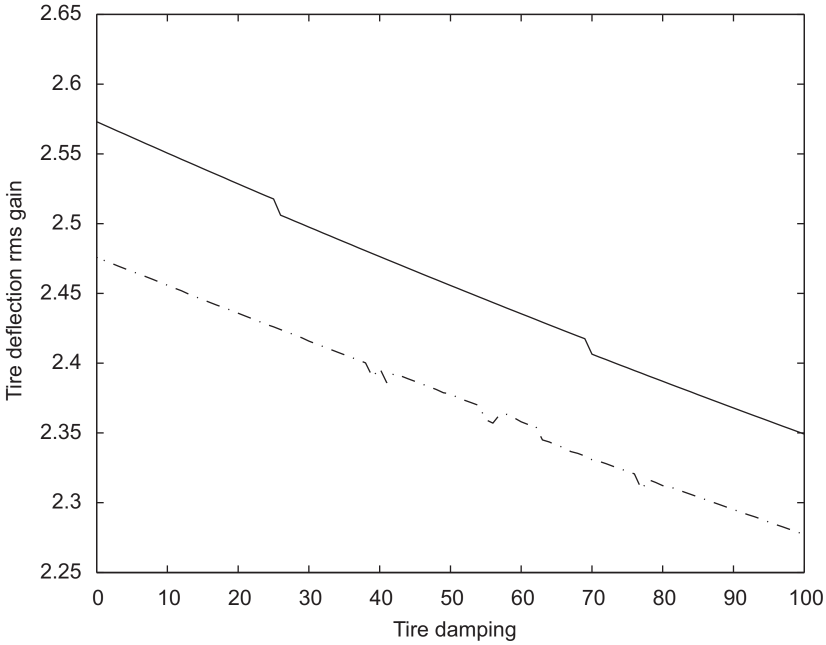

Fig. 9. $\|\mathscr{W}\mathbf{T}_{\mathbf{zw}}\|_\infty$ as a function of c_t: (-) passive suspension; (-.) active suspension with $\rho_1 = 1$ and $\rho_2 = 1$ using the suspension travel measurements.

design using linear matrix inequalities. For a given range of tire damping coefficients, it was observed that only road-holding quality was influenced to some extent by tire damping while the rest of the responses were slightly affected. In addition, precise knowledge of tire damping is an unrealistic assumption. In the next

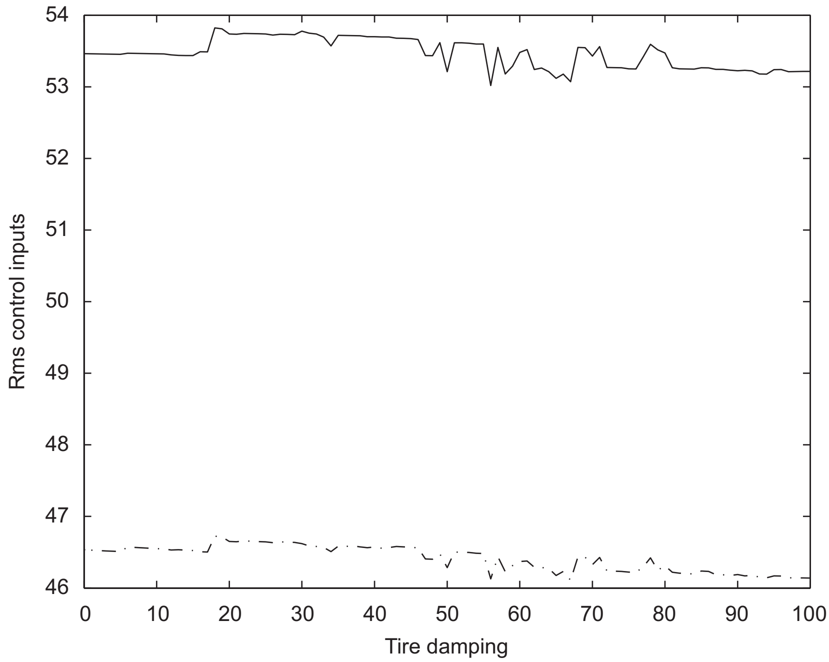

Fig. 10. The rms values of the actuator forces as functions of c_t: (-) u_1; (-.) u_2 with $\rho_1 = 1$ and $\rho_2 = 1$ using the suspension travel measurements.

subsection, this assumption will be relaxed and a robust multi-objective suspension control problem will be formulated.

3.2. Polytopic vehicle suspension models

The multi-objective control problem solved in Section 3.1 assumes exact values of the tire damping coefficients, which are difficult to estimate since they depend on many factors and vary during ride. In this subsection, assuming that c_{tk}, $k = 1, 2$ take values in some prescribed intervals $[\alpha_k, \beta_k]$ a multi-objective controller with guaranteed performance for all possible values of tire damping coefficients will be designed. Note that this uncertainty structure allows fast variations of the tire damping coefficients.

Let $\mathbf{A}^0$ and $\mathbf{B}_1^0$ denote the matrices $\mathbf{A}$ and $\mathbf{B}_1$ in Eqs. (7) and (8) evaluated at $c_{t1} = c_{t2} = 0$ and let $\mathbf{A}^k = \mathrm{d}\mathbf{A}/\mathrm{d}c_{tk}$, $\mathbf{B}_1^k = \mathrm{d}\mathbf{B}_1/\mathrm{d}c_{tk}$, $k = 1, 2$. Define three vertex systems by the quadruplets $\mathscr{P}_0 = (A^0, [B_1^0 \;\; B_2], [C_1; C_2], [0 \; D_1; 0 \; 0])$ and $\mathscr{P}_k = (A^k, [B_1^k \; 0], 0, 0)$, $k = 1, 2$. Then, the quadruplet $\mathscr{P}$ formed conformally with $\mathscr{P}_0$, $\mathscr{P}_1$, and $\mathscr{P}_2$ and describing the system studied in Section 3.1 can be written as

$$\mathscr{P} = \mathscr{P}_0 + c_{t1}\mathscr{P}_1 + c_{t2}\mathscr{P}_2, \quad c_{tk} \in [\alpha_k, \beta_k], \;\; k = 1, 2, \tag{19}$$

which is a box in the Euclidean space of the state-space parameters. Then, the robust multi-objective control design problem is:

For given numbers $\gamma > 0$, $\Lambda_k = 0$ *for* $k = 3, 4$ *and* $\Lambda_k > 0$ *otherwise and all* $\mathscr{P}$ *in Eq.* (19), *design a state-feedback controller* $\mathbf{u} = \mathbf{F}_0\tilde{\mathbf{x}}$ *that satisfies* $\|\mathscr{W}\mathbf{T}_{\mathbf{zv}}\|_\infty < \gamma$ *and minimizes* $\|\mathbf{\Lambda}\mathbf{T}_{\mathbf{zv}}\|_2^2$.

Again, this optimization problem can be solved by using linear matrix inequalities. Its solution is implemented by the `msfsyn` command in MATLAB's LMI Toolbox [22]. For illustration, suppose $\alpha_k = 0$ and $\beta_k = 100$ for $k = 1, 2$. The same formulas for Λ_k, $k = 1, \ldots, 6$ and γ proposed in Section 3.1 can be used provided that the scalings $\|\mathbf{G}_{z_k\mathbf{v}}\|$ are computed with fixed c_{t1} and c_{t2}. For the computations, $c_{t1} = c_{t2} = 0$ were picked and the above optimization problem was solved. Let $\mathbf{F}_0$ denote the solution which depends on the scalings ρ_1 and ρ_2. Using the same msfsyn command with the uncertainty set $\mathscr{P}_0$, which is a singleton, and the same weights, another controller denoted by $\bar{\mathbf{F}}_0$ was obtained.

In order to see how the robust controller is performing against $\bar{\mathbf{F}}_0$, fix c_{t1} and c_{t2} and denote the corresponding system in Eq. (19) by $\mathscr{P}_t$. Then, compute the closed-loop responses of $\mathscr{P}_t$ using the controllers $\bar{\mathbf{F}}_0$ and $\mathbf{F}_0$ with a range of values for ρ_1 and ρ_2. It has been observed that the two response sets are almost identical in all cases. For example, when $\rho_1 = \rho_2 = 1$, the rms vertical accelerations are 0.10145 with $\mathbf{F}_0$ and 0.10160 with $\bar{\mathbf{F}}_0$ corresponding to $c_{t1} = c_{t2} = 100$. The last result suggests neglecting tire damping in the design of active suspension systems for half-car models when it is difficult to estimate tire damping coefficients.

4. Conclusions

In this paper, multi-objective control of a half-car suspension system using linear matrix inequalities was studied. It was observed that when the tire damping coefficients are precisely estimated, their values affect to some extent only road-holding quality. In the absence of this information, a robust controller was synthesized for a suspension system with polytopic tire damping uncertainties. This robust controller synthesis was seen not to offer any advantage over an active suspension system designed by neglecting tire damping. The last result is in sharp contrast with a conclusion in Ref. [23] drawn for a robustly controlled quarter-car active suspension system. A possible mechanism for this discrepancy is the body pitch which does not allow decomposition of the half-car model in Fig. 1 into two independent quarter-car models by coupling their vertical motions. In a multi-input/multi-output framework, the study of achievable performance for half-car active suspensions remains future work.

References

[1] A.G. Thompson, Design of active suspensions, *Proceedings of the Institution of Mechanical Engineers* 185 (1970–1971) 553–563.
[2] D. Hrovat, D.L. Margolis, M. Hubbard, An approach toward the optimal semi-active suspension, *Transactions of the ASME, Journal of Dynamic Systems, Measurement, and Control* 110 (1988) 288–296.
[3] A. Alleyne, J.K. Hedrick, Nonlinear adaptive control of active suspensions, *IEEE Transactions on Control Systems Technology* 3 (1995) 94–101.
[4] M. Yamashita, K. Fujimori, K. Hayakawa, H. Kimura, Application of H_∞ control to active suspension systems, *Automatica* 30 (1994) 1717–1729.
[5] D. Karnopp, Active and semi-active vibration isolation, *Transactions of the ASME, Journal of Mechanical Design* 117B (1995) 177–185.
[6] H.D. Tuan, E. Ono, P. Apkarian, Nonlinear H_∞ control for an integrated suspension system via parameterized linear matrix inequality characterizations, *IEEE Transactions on Control Systems Technology* 9 (2001) 175–185.
[7] I. Fialho, G.J. Balas, Road adaptive suspension design using linear parameter-varying gain scheduling, *IEEE Transactions on Control Systems Technology* 10 (2002) 43–54.
[8] H. Chen, K.H. Guo, Constrained H_∞ control of active suspensions: an LMI approach, *IEEE Transactions on Control Systems Technology* 13 (2005) 412–421.
[9] D. Karnopp, Theoretical limitations in active suspensions, *Vehicle System Dynamics* 15 (1986) 41–54.
[10] C. Yue, T. Butsuen, J.K. Hedrick, Alternative control laws for automotive active suspensions, *Transactions of the ASME, Journal of Dynamic Systems, Measurement, and Control* 111 (1989) 286–291.
[11] J.K. Hedrick, T. Butsuen, Invariant properties of automotive suspensions, *Proceedings of the Institution of Mechanical Engineers, Part D, Transport Engineering* 204 (1990) 21–27.
[12] M.C. Smith, Achievable dynamic response for automotive active suspensions, *Vehicle System Dynamics* 24 (1995) 1–34.
[13] M.C. Smith, G.W. Walker, Performance limitations and constraints for active and passive suspensions: a mechanical multi-port approach, *Vehicle System Dynamics* 33 (2000) 137–168.
[14] S. Türkay, H. Akçay, Aspects of achievable performance for quarter-car active suspensions, *Journal of Sound and Vibration* 311 (2008) 440–460.
[15] H.B. Pacejka, *Tyre and Vehicle Dynamics*, second ed., Butterworth-Heinemann, Burlington, MA, 2006.
[16] G. Jianmin, R. Gall, W. Zuomin, Dynamic damping and stiffness characteristics of the rolling tire, *Tire Science and Technology* 29 (2001) 258–268.
[17] J.A. Levitt, N.G. Zorka, Influence of tire damping in quarter car active suspension models, *Transactions of the ASME, Journal of Dynamic Systems, Measurement, and Control* 113 (1991) 134–137.
[18] C. Papageorgiou, M.C. Smith, Positive real synthesis using matrix inequalities for mechanical networks: application to vehicle suspension, *IEEE Transactions on Control Systems Technology* 14 (2006) 423–435.
[19] J. Wang, D.A. Wilson, Mixed $GL_2/H_2/GH_2$ control with pole placement and its application to vehicle suspension systems, *International Journal of Control* 74 (2001) 1353–1369.

[20] H. Chen, P.Y. Sun, K.H. Guo, A multi-objective control design for active suspensions with hard constraints, *Proceedings of the American Control Conference*, vol. 1, 2003, pp. 4371–4376.

[21] H. Gao, J. Lam, C. Wang, Multi-objective control of vehicle active suspension systems via load dependent controllers, *Journal of Sound and Vibration* 290 (2006) 654–675.

[22] P. Gahinet, A. Nemirowski, A.J. Laub, M. Chilali, *LMI Control Toolbox*, first ed., The Mathworks, Natick, MA, 1995.

[23] H. Akçay, S. Türkay, RMS performance limitations and constraints for quarter-car active suspensions, *Proceedings of the 16th Mediterranean Conference on Control and Automation*, Ajaccio, Corsica, France, June 2008, pp. 425–430.

[24] S. Türkay, H. Akçay, Influence of tire damping on the $\mathscr{H}_2$ optimally designed half-car active suspension, *Proceedings of the 2008 IEEE Multi-conference on Systems and Control*, San Antonio, Texas, September 2008, pp. 444–449.